ISSN 2070-2051, Protection of Metals and Physical Chemistry of Surfaces, 2023, Vol. 59, No. 5, pp. 860–867. © Pleiades Publishing, Ltd., 2023.
Russian Text © The Author(s), 2023, published in Fizikokhimiya Poverkhnosti i Zashchita Materialov, 2023, Vol. 59, No. 5, pp. 522–529.

PHYSICOCHEMICAL PROCESSES AT THE INTERFACES

Synthesis and Sorption Properties of Lithium Aluminosilicate

P. S. Gordienko[a], E. V. Pashnina[a], S. B. Yarusova[a, b, *], E. A. Nekhlyudova[a, b], I. G. Zhevtun[a], I. A. Shabalin[a], N. V. Zarubina[c], S. Yu. Budnitsky[c], and V. G. Kuryavyi[a]

[a] *Institute of Chemistry, Far Eastern Branch, Russian Academy of Sciences, Vladivostok, 690022 Russia*

[b] *Vladivostok State University, Vladivostok, 690014 Russia*

[c] *Far Eastern Geological Institute, Far Eastern Branch, Russian Academy of Sciences, Vladivostok, 690022 Russia*

**e-mail: yarusova_10@mail.ru*

Received April 17, 2023; revised June 17, 2023; accepted June 17, 2023

Abstract—The article presents data on the synthesis of nanostructured, X-ray amorphous lithium aluminosilicate, with a Si : Al ratio of 3 : 1. The composition, morphology, and thermal behavior were studied. The sorption isotherm of Cs^+ ions was obtained under static conditions with a ratio of T : L = 1 : 400. The maximum sorption capacity, degree of extraction, and distribution coefficients of cesium were determined. Data on the sorption kinetics of Cs^+ ions were obtained at temperatures 30 and 60°C, and the activation energy of the sorption process and diffusion coefficients were calculated.

Keywords: lithium aluminosilicate, synthesis, sorption properties, cesium, kinetics, activation energy, diffusion coefficients

DOI: 10.1134/S2070205123701046

INTRODUCTION

An effective solution to environmental problems associated with the purification of, first of all, water areas from long-lived radioisotopes of cesium, strontium, and a number of heavy metals, involves the active search for both new types of materials and synthesis of sorbents of a known class, but under conditions that make it possible to obtain a material with a given composition, a certain dispersion, and improved functional properties. The relevance of such research became obvious in connection with a number of environmental disasters that occurred at nuclear power plants and nuclear materials processing plants from the mid-1960s to the present day.

The modern nuclear energy cycle for electricity production requires highly efficient radionuclide sorbents and matrices based on them, which have a set of physicochemical and mechanical characteristics: both high resistance to mechanical loads and high chemical and radiation resistance in various environments under conditions of long-term disposal of highly active nuclear waste. Silicates and aluminosilicates satisfy these requirements and therefore belong to in-demand natural and synthetic minerals widely used as sorbents of toxic substances in liquid and gaseous media, and as catalysts in the production of various types of hydrocarbons, in medicine, etc. [1–4]. Natural and synthetic aluminosilicates (zeolites, clays), as well as composite materials created with them, occupy a particular place among inorganic materials for extraction of radionuclides ^{90}Sr, ^{137}Cs, and other isotopes from process waters [5–9].

Earlier, at the Institute of Chemistry, Far Eastern Branch, Russian Academy of Sciences (IC FEB RAS), nanostructured aluminosilicates of alkali and alkaline earth metals with a specific surface area of 30–300 $m^2\ g^{-1}$ and high sorption capacity values with respect to Cs^+ and Sr^{2+} were synthesized from aqueous multicomponent systems. Researchers have studied such classes of compounds as potassium and sodium aluminosilicates $Me_xAl_xSi_{at}O_{(2y + 2x)}\cdot nN_2O$ (where Me = K^+,Na^+), calcium and barium aluminosilicates and silicates ($MeAl_2Si_nO_{(n + 2)2}\cdot mH_2O$; $MeO\cdot nSiO_2\cdot mH_2O$ (where Me = Ca^{2+}, Ba^{2+}) [10–16].

Given the previously obtained results on the synthesis and sorption characteristics of the synthetic compound $KAlSi_3O_8\cdot 1.5H_2O$ [10], using spark plasma sintering, solid-state matrices were synthesized based on amorphous $KAlSi_3O_8\cdot 1.5H_2O$ and potassium aluminosilicate from plant waste saturated with cesium to immobilize of cesium-137. For the first time, samples of solid matrices based on ($(Cs,K)AlSi_3O_8$) with a high relative density, compressive strength, and Vickers microhardness were obtained. Their high hydrolytic stability has been proven (within 10^{-7} g cm^{-2} $days^{-1}$) and low diffusion coefficient D_e of cesium during leaching from the volume of matrices (within the lim-

its) 7.36×10^{-9} and 9.07×10^{-14} cm^2 s^{-1} for model ($(Cs,K)AlSi_3O_8$) – matrices and RS-$(K,Cs)AlSi_3O_8$ – matrices (from rice straw), respectively. The high quality of the resulting products has been confirmed in accordance with GOST R 50926-96 and existing analogues, which is of practical interest for technologies for purifying and processing radioactive waste and creating radioisotope products [17, 18].

Because nanostructured aluminosilicates of alkali and alkaline earth metals have a high sorption capacity with respect to cesium ions, we made an assumption about the effectiveness of using lithium aluminosilicates. It should be noted that the bulk of the literature on lithium silicates is devoted to the synthesis of these compounds and their use for the production of, e.g., lithium aluminosilicate glass ceramics, lithium ion sieves for extracting lithium from low-grade brines, CO_2 sorbents, etc. [19–23].

The objective of this article was to synthesize and study the composition, morphology, thermal behavior, and sorption properties under static conditions of nanostructured lithium aluminosilicate with a Si/Al ratio of 3 : 1 with respect to cesium ions.

EXPERIMENTAL

Synthesis of Lithium Aluminosilicate

Lithium aluminosilicate with a given Si/Al ratio was synthesized according to the reaction

$$4LiOH + 3SiO_2 \cdot nH_2O + AlCl_3 \cdot 6H_2O \rightarrow LiAlSi_3O_8 + 3LiCl + 11H_2O. \quad (1)$$

At the first stage, liquid lithium glass with a silicate modulus of 1.5 was obtained:

$$4LiOH + 3SiO_2 \rightarrow Li_4Si_3O_8 + H_2O. \quad (2)$$

Then an aluminum chloride solution was added to the resulting solution with constant stirring.

The ratio of components corresponded to Eq. (1), and the pH of the solution at the end of the synthesis process had a neutral value (pH 7). For the synthesis, the following reagents were used: lithium hydroxide (GOST 8595–83), grade MKU-85 finely dispersed silica (condensed microsilica TU 5743-048-02495332-96), and reagent grade aluminum chloride hexahydrate (TU STP COMP 2-191-10). Lithium hydroxide was dissolved in distilled water, which was had been preboiled to remove dissolved CO_2 molecules to prevent lithium carbonate formation.

The resulting lithium aluminosilicate precipitate was separated from the solution through a blue ribbon filter, washed with distilled water until the reaction to chlorine ions was negative, and dried at a temperature of 110°C.

Cs^+ Sorption Experiments

Cs^+ sorption experiments were carried out under static conditions at a ratio of the solid and liquid phases of 1 : 400 and a temperature of 20°C from aqueous solutions of cesium chloride without a salt background with different initial concentrations of Cs^+ ions from 0.5 to 106.8 mmol L^{-1} with stirring on an RT 15 power magnetic stirrer (IKA WERKE, Germany) for 3 h.

Cs^+ sorption kinetics experiments were carried out under static conditions at a ratio of the solid and liquid phases of 1 : 400 and temperatures of 30 and 60°C from aqueous solutions of cesium chloride without a salt background with an initial concentration of Cs^+ 3.35 mg L^{-1} in an interval of 3–20 min.

Analysis Methods

XRD patterns of the samples were taken on a D8 ADVANCE automatic diffractometer (Germany) with sample rotation in CuK_α radiation. XRD was performed in the EVA search program with the PDF-2 powder data bank.

To quantitatively determine the elemental composition of the synthesized aluminosilicates, the energy-dispersive X-ray fluorescence method was used using a Shimadzu EDX 800 HS spectrometer (Japan). A weighed portion of the sample was ground in an agate mortar with boric acid (2 : 1 by weight) and placed in a mold with a diameter of 20 mm. The source tablet was pressed for 2 min at a pressure of 5000 kg, after which it was placed in a spectrometer and measurements were taken. The exposure time was 100 s in each energy channel, the radiation source was an X-ray tube with a Rh anode, and the element concentrations were calculated using the fundamental parameters method using the spectrometer software package without taking light elements into account. The relative error in determining the elemental composition did not exceed ±10%.

The lithium content in the sample was determined using inductively coupled plasma mass spectrometry (ICP-MS) with subsequent conversion to molar content. To preliminarily transfer the sample into a soluble state, a sample of the substance was treated with a hot hydrofluoric acid solution to remove silicon in the form SiF_4. Next, a solution of wet salts of lithium fluoride (LiF) and aluminum fluoride (AlF_3) was boiled in a solution of 1N hydrochloric acid to convert fluorides into soluble $AlCl_3$ and LiCl salts, as well as to remove traces of fluorine from the solution. Next, the solutions were transferred into polypropylene volumetric flasks for subsequent ICP-MS analysis.

Thermogravimetric analysis was carried out with Q-1500 D derivatograph of the F. Paulik, P. Paulik, L. Erdei system (MOM< Hungary) (temperature determination accuracy ±5°C), with firing of samples

up to 900°C at a rate of 10°C/min in an open platinum crucible in air.

The specific surface area of the samples was determined by low-temperature nitrogen adsorption using a Sorbtometer-M device (Russia).

The density of aluminosilicates was determined with a pycnometer.

The morphology of the samples was studied with a HitachiS5500 high-resolution scanning electron microscope (Japan). Before imaging, the samples were coated with a conductive layer of platinum. The shooting was carried out at an accelerating voltage of 7 kV and a vacuum of 10^{-5} Torr.

The concentrations of Li^+ and Cs^+ in the analyzed solutions were determined by ICP-MS on an Agilent 8800 spectrometer (Agilent Technologies, USA, 2013) with a relative error no greater than 10%. Prior to measurements, the solutions were diluted 100 times. The following analytical isotopes were selected for analysis: ^{7}Li and ^{133}Cs.

To calibrate the device, a multielement certified solution ICP-MS Verification Standard E (High Purity Standards, USA) was used. The ICP-MS detection limit (DL) was for Li 0.07 μg dm^{-3}; for Cs, 0.03 μg dm^{-3}.

The sorption capacity (A_c, mmol g^{-1}) of the studied samples were calculated by the formula

$$A_c = \frac{(C_{init} - C_{eq})}{m}V, \quad (3)$$

where C_{init} is the initial concentration Cs^+ ions in solution, mmol L^{-1}; C_{eq} is the equilibrium concentration of Cs^+ ions in solution, mmol L^{-1}; V is the volume of the solution, L; m is the mass of the sorbent, g.

The extraction rate of Cs^+ ions (α, %) was calculated by the formula

$$\alpha = \frac{(C_{init} - C_{eq})}{C_{init}} \times 100\%. \quad (4)$$

The interphase distribution coefficient (K_d, mL g^{-1}) was determined as follows:

$$K_d = \frac{(C_{init} - C_{eq})V}{C_{eq}m}. \quad (5)$$

RESULTS AND DISCUSSION

XRD of the resulting sample before and after firing (Fig. 1) showed that the resulting compound is X-ray amorphous, as evidenced by a blurred peak characteristic of amorphous substances in the angle range of 15°–35°. It can be seen that when the sample is heated to 1000°C (Fig. 1, *b*), partial crystallization occurs, accompanied by the appearance of peaks in the XRD pattern and a shift in the halo maximum. However, it was not possible to assign the detected peaks to a specific crystalline phase.

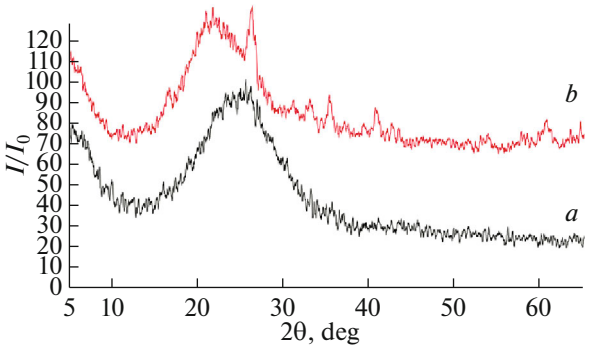

Fig. 1. X-ray diffraction pattern of lithium aluminosilicate sample: (*a*) initial sample after drying at 110°C, (*b*) sample after firing at 1000°C.

According to X-ray fluorescence analysis, the contents of Si and Al are 74.9 and 24.8 wt %, respectively; i.e., the actual ratio Si/Al = 3 : 1, which corresponds to the given ratio during synthesis (silicon content 2.7 mol; aluminum content, 0.9 mol). According to the ICP-MS data, the lithium content in the sample is 4.38 wt %, or is 0.63 mol.

The thermogravigram in Fig. 2 shows that the gradual dehydration of synthetic lithium aluminosilicate occurs in the temperature range of 30–500°C and is characterized by a broadened endoeffect. Removal of adsorption water occurs up to 110°C (this is a rather arbitrary value) and is accompanied by a loss in weight of 15.6%. The total loss in weight is 37.2%. Excluding weight loss due to adsorption water, 21.6% of the weight loss is due to bound crystallization water, which corresponds to 4.7 H_2O molecules. The gross formula of the resulting compound was calculated from the results of energy-dispersive X-ray fluorescence, ICP-MS, and thermogravimetric analysis: $Li_{0.63}H_{0.27}Al_{0.9}Si_{2.7}O_8 \cdot 4.7H_2O$.

The specific surface area of the sample is 132.0 $m^2\ g^{-1}$. The density of the resulting sample is 2.5 g cm^{-3}.

Figure 3 shows SEM images of lithium aluminosilicate after drying (initial sample).

Aluminosilicate has a loose layered structure characteristic of clays and clay minerals such as kaolinite, montmorillonite, sepiolite, palygorskite, vermiculite, etc. (Figs. 3, 4a).

When the initial sample is heated to 1000°, the morphology of the observed surface changes significantly. Numerous pores with a diameter no greater than 20–100 nm are formed (Fig. 4b).

To assess the sorption properties, the resulting isotherm was analyzed in coordinates of the Langmuir equation and empirical Freundlich equation.

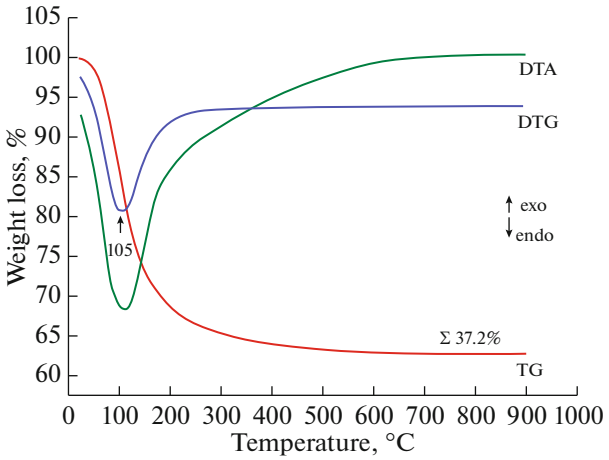

Fig. 2. Thermogravigram of lithium aluminosilicate sample.

Langmuir equation:

$$\frac{C_{eq}}{A_c} = \frac{1}{A_{max}k} + \frac{C_{eq}}{A_{max}}, \quad (6)$$

where C_{eq} is the equilibrium concentration of Cs^+ ions in solution, A_{max} is the maximum sorption capacity, and k is the Langmuir constant.

The constant of the equation was calculated from the slope and intercept of the line on the graph at the corresponding coordinates of the linear equation C_{eq}/A_c from C_{eq}: $y = 0.1613x$ 6.0617 ($R^2 = 0.8516$). The found parameters of the Langmuir equation are: A_{max} = 6.2 mmol g^{-1}, $k = 0.03$ L $mmol^{-1}$, taking into account the measurement error of Cs^+ concentrations within 10–15% using ICP-MS, experimental data on the maximum sorption capacity and calculated using the Langmuir equation of the same order.

The obtained high maximum sorption capacity can be explained by the morphology of lithium aluminosilicate, high specific surface area (greater than 130 m^2 g^{-1}) and high chemical affinity of cesium and lithium.

Table 1 presents the dependence of the coefficient of the interphase distribution of cesium on lithium aluminosilicate and the degree of extraction of Cs^+ ions on the ratio of solid and liquid phases.

It follows that at T : L = 1 : 40, the degree of extraction of Cs^+ ions reaches 97%, and the highest value of the distribution coefficient is observed at the ratio T : L = 1: 2000 (K_d 0.74 × 10^4 mL g^{-1}). Taking into account the thermochemical properties of the sorbent based on lithium aluminosilicate, it is possible to form compounds for effective extraction of cesium with subsequent thermomechanical treatment of the sorbent with the sorbed isotope.

Kinetics of the Sorption Process

In Fig. 6 shows the kinetic curves of sorption of Cs ions+ lithium aluminosilicate at temperatures 30 and 60°C.

As can be seen from the presented kinetic curves, the sorption capacity reaches a maximum within 10 min, increasing with increasing temperature.

To describe the kinetics of topochemical reactions, which include the process under study, we used the equation substantiated in [24]:

$$A_{curr} = A_{max}kt\frac{1}{1+kt}, \quad (7)$$

where k is a dimensional constant $(time)^{-1}$; t is the sorption time; A_{curr} and A_{max}–current and maximum sorption capacity.

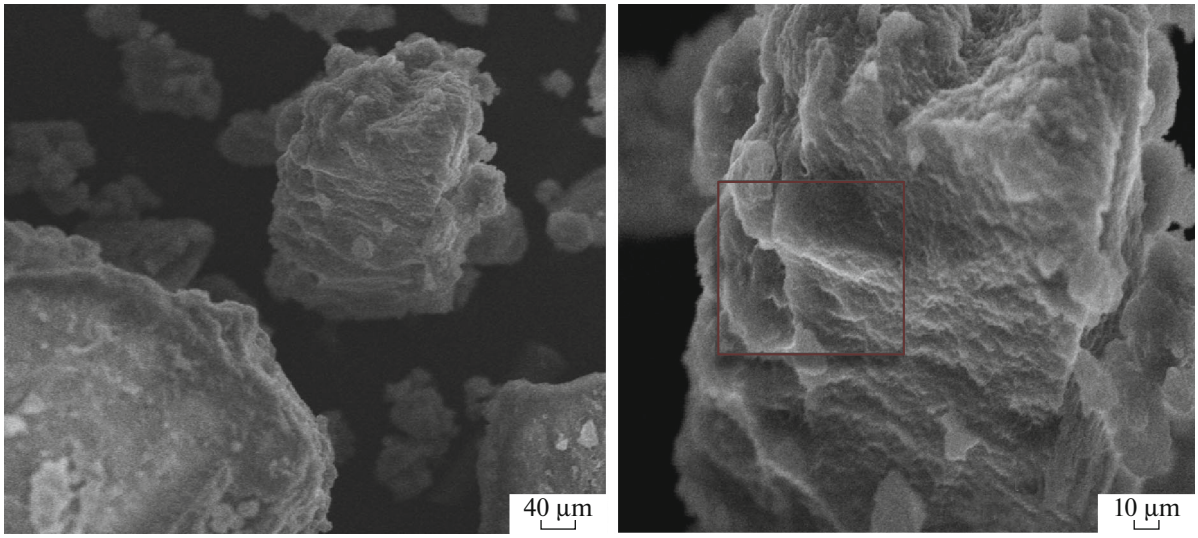

Fig. 3. SEM images of lithium aluminosilicate particles (initial sample).

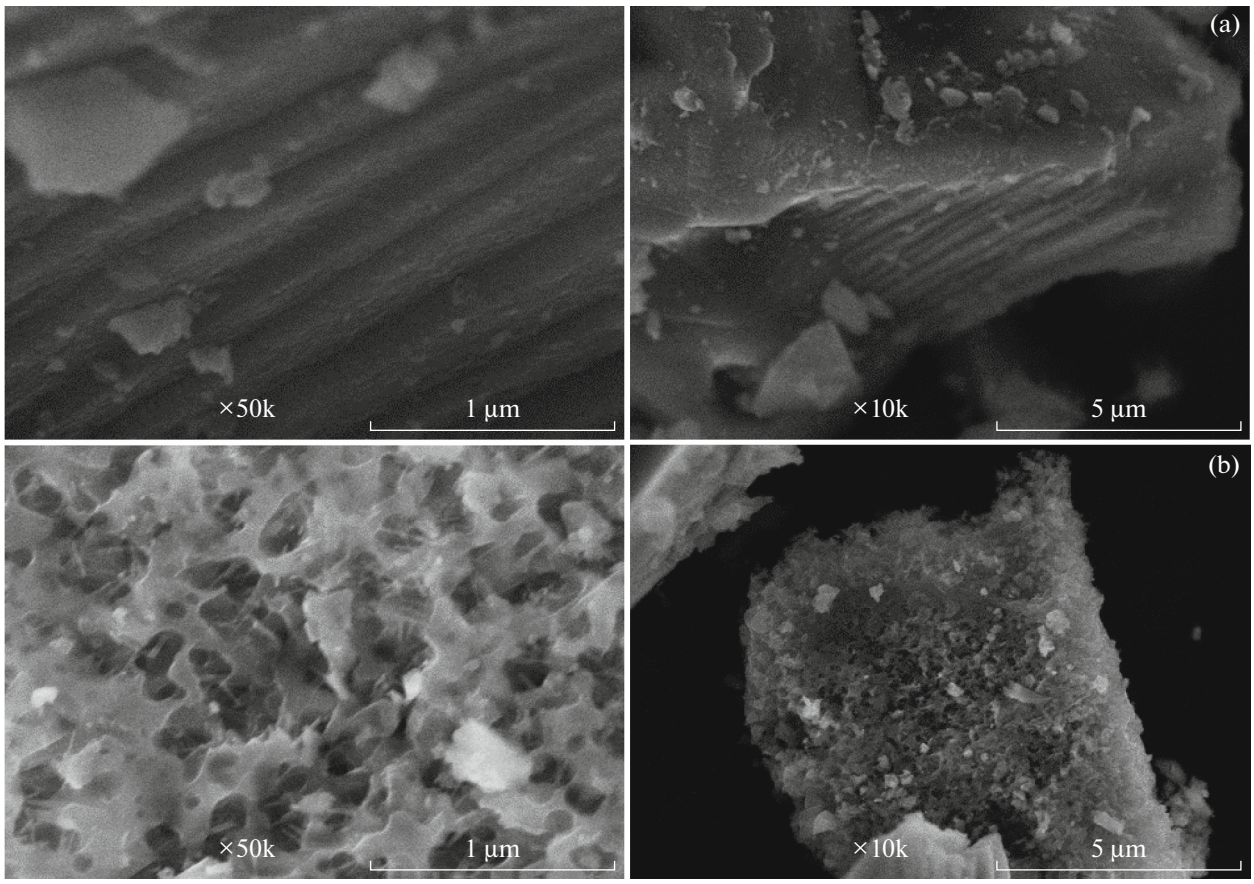

Fig. 4. SEM images of lithium aluminosilicate particles: (a) initial sample; (b) after firing at 1000°C.

To determine the constant k and A_{max}, Eq. (7) is transformed into a straight line equation of the form ($y = A\ bx$):

$$\frac{1}{A_{curr}} = \frac{1}{A_{max}} + \frac{1}{ktA_{max}},\ (a = 1/A_{max};b = 1/(A_{max}k)). \quad (8)$$

Linear kinetic equations were obtained for different sorption temperatures (Figs. 7a, 7b): $y = 154.02X$ 150.45, $R^2 = 0.8313$ (30°C); $y = 227.69X$ 108.91, $R^2 =$ 0.9291 (60°C), and the k values are determined from the equations, which are of 0.98 and 0.478 min^{-1} for the corresponding temperatures. The calculated values of the maximum sorption capacity A_{max} are 6.65×10^{-3} mmol g^{-1} for 30°C and 9.2×10^{-3} mmol g^{-1} for 60°C.

Knowing the constants of the sorption process at two temperatures ($K_{t1} = 0.98\ min^{-1}$, $K_{t2} = 0.478\ min^{-1}$), we determined the activation energy of the sorption process by this sorbent using the Arrhenius equation:

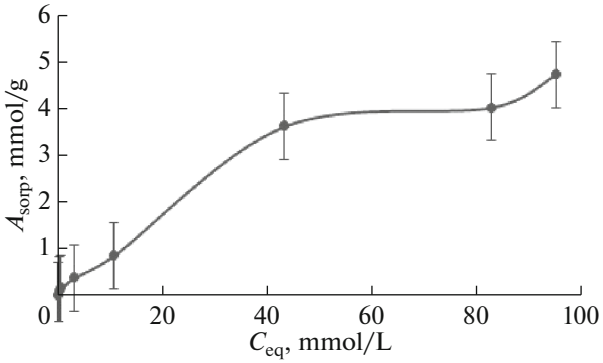

Fig. 5. Isotherms of Cs^+ sorption by lithium aluminosilicate.

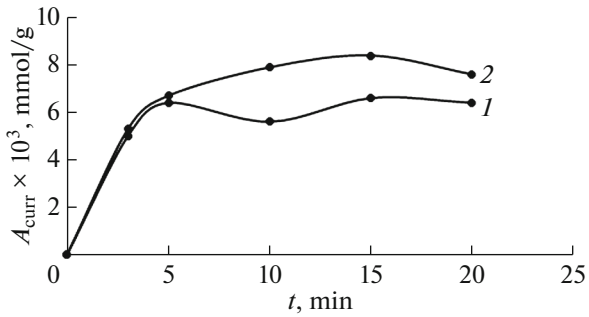

Fig. 6. Kinetic dependences of the sorption of Cs^+ ions by lithium aluminosilicate at various temperatures: (*1*) 30; (*2*) 60°C.

Table 1. Values of sorption capacity, degree of extraction α, (%), and K_d of cesium ions at different values of T : L ($t = 20$°C, initial concentration of Cs^+ ions 3.35 mg/L (25.2 μmol/L))

T : L	K_d, mL/g	$A_{sorp} \times 10^{-3}$, mmol/g	a, %
1 : 40	1215	0.52	96.8
1 : 100	1457	0.993	93.6
1 : 400	2550	4.04	86.8
1 : 1000	1735	12.6	64.6
1 : 2000	7339	52.3	79.7

$$\ln(K_{t1}/K_{t2}) = (Q/R)(1/T_2 - 1/T_1), \quad (9)$$

where Q is the activation energy, kJ mol^{-1} and R is the gas constant, 8.314 J mol^{-1} K^{-1}. The activation energy of the sorption process, calculated from the experimental data, is 19.98 kJ mol^{-1}.

From the obtained values of the constants K_{t1} = 0.98 min^{-1} (for 30°C) and K_{t2} = 0.478 min^{-1} (for 60°C) and from Eq. (7), it follows that at a sorption time of the reciprocal of the constant ($t = 1/K_t$), the sorption capacity should reach a value of half the maximum value, but from the experimental data on the value of the sorption capacity over time, it follows that already with a minimum sorption time of 3 min, the sorption capacity reaches 70–80% of the sorption capacity determined for the sample at 20 min of sorption and is taken as the equilibrium maximum value (Fig. 6). It was assumed that during the sorption time within 20 min at temperatures of 30 and 60°C, thermodynamic equilibrium is established and the equilibrium constants of cation exchange K_{eq} can be determined as the ratio of the equilibrium concentration of Cs^+ ions at the appropriate temperature (1.19 mg L^{-1} for 30°C and 0.77 mg L^{-1} for 60°C) to the initial concentration of 3.35 mg L^{-1}. The following values of the constants were obtained: 0.358 and 0.23, respectively, for the indicated temperatures.

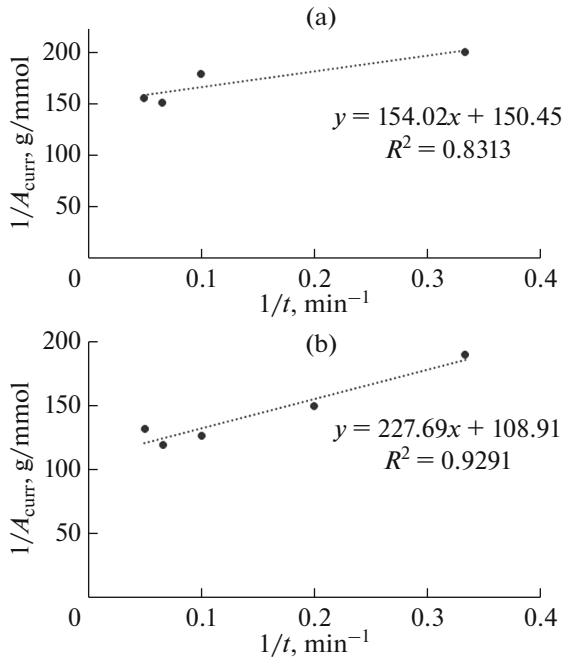

Fig. 7. Dependence of reciprocal value of sorption capacity of lithium aluminosilicate $1/A_{curr}$ on $1/t$ at different temperatures: (a) 30, (b) 60°C.

Applying empirical laws to calculate changes in isobaric-isothermal potential Δg using the Gibbs–Helmholtz equation,

$$\Delta G = \Delta H_T - T\Delta S, \quad (10)$$

and the (van't Hoff) dependence of this potential on the logarithm of the equilibrium constant,

$$\Delta G = RT \ln K_{eq}, \quad (11)$$

these equilibrium constants for these temperatures are presented as a dependence:

$$\ln K_{eq} = -\Delta H_T/TR + \Delta S/R, \quad (12)$$

we obtain the equation $y = 1.4332x - 0.0017$, from which it follows that sorption by this sorbent in the studied temperature range is accompanied by a slight change in the entropy of the system $\Delta S = -0.014$ J mol^{-1} K^{-1}, enthalpy $\Delta H = -11.9$ J mol^{-1}, and free energy $\Delta g = -7.28$ J mol^{-1}.

To draw a conclusion about the diffusion parameters of the sorption of Cs^+ ions with a specific nanostructured sorbent, the methodology and calculation equations given in [25] for highly dispersed materials were used:

$$\Upsilon_{curr} = \Upsilon_o + (2S/V)(\sqrt{t}\sqrt{D})/\sqrt{\pi}, \quad (13)$$

where Υ_{curr}, A_{curr}/A_{max} is the relative value of sorption; S is the specific surface area of the sorbent, cm^2 g^{-1}; V is the volume of the sorbent sample, cm^3 ($V = m/\rho$, where m is the sorbent mass, g; ρ is the sorbent density, g cm^{-3}); t is time, s; D is the diffusion coefficient, cm^2 s^{-1}; $\pi = 3.14$.

When this approach is used, experimental data is required on a value of Υ_{curr} less than 0.5, but such relative sorption values are possible at sorption times $t < 1/K_{curr}$, according to Eq. (7), and it is difficult to obtain them experimentally. However, using Eq. (8) and the values $A_{max} = 6.65 \times 10^{-3}$ mmol g^{-1}, $K_{t1} = 0.98$ min^{-1} (for 30°C); and $A_{max} = 9.2 \times 10^{-3}$ mmol g^{-1}, $K_{t2} = 0.478$ min^{-1} (for 60°C), determined from the experimental data, we obtained the Υ values by calculating $\Upsilon_{curr} = A_{curr}/A_{max}$ at times $t < 1/K_{curr}$ (Table 2).

According to the data presented in Table 2, we plotted the dependences $\Upsilon_{curr} = f(\sqrt{t})$ shown in Fig. 8 and obtained the straight line equations $y = 0.0736x - 0.0786$, $R^2 = 0.99$ and $y = 0.0462x - 0.0548$, $R^2 = 0.9769$ for temperatures of 30 and 60°C, respectively.

Table 2. Data for calculating diffusion coefficient

$t = 30°C$, $A_{max} = 6.65 \times 10^{-3}$ mmol g^{-1}				$t = 60°C$, $A_{max} = 9.2 \times 10^{-3}$ mmol g^{-1}			
t, s	$A_{curr} \times 10^3$, mmol g^{-1}	$\sqrt{t}$, s$^{1/2}$	$\Upsilon_{curr} = A_{curr}/A_{max}$	t, s	$A_{curr} \times 10^3$, mmol/g	$\sqrt{t}$, s$^{1/2}$	$\Upsilon_{curr} = A_{curr}/A_{max}$
61.2	3.17	7.82	0.499	125	4.58	11.18	0.49
50	2.85	7.07	0.449	100	4.07	10	0.44
25	1.84	5.0	0.289	50	2.61	7.07	0.28
15	1.24	3.87	0.196	30	1.77	5.47	0.19
10	0.89	3.16	0.140	15	0.98	3.87	0.106
3	0.29	1.73	0.046	5	0.35	2.23	0.038
2	0.2	1.41	0.031	1	0.07	1	0.007

The angular coefficients for x in accordance with Eq. (13) are $(2S/V)\sqrt{D}/\sqrt{\pi} = 0.0736$ for 30°C and 0.0462 for 60°C. All data for calculating the diffusion coefficient are determined: the volume of sorbent V is calculated ($m = 0.05$ g, density 2.5 g cm^{-3}), specific surface area 132 m^2 g^{-1}. The diffusion coefficients for Cs^+ ions calculated using the described method are 3.81×10^{-16} and 1.53×10^{-16} cm^2 s^{-1} for 30 and 60°C, respectively.

Taking into account the initial and equilibrium value of the sorbate concentration in the solution in Eq. (13), we can take into account the coefficient N, which is equal to their ratio C_{int}/C_{eq} (3.35 mg L^{-1} is the initial concentration, 1.18 mg L^{-1} is the equilibrium concentration at 30°C, and 0.766 mg L^{-1} at 60°C):

$$\Upsilon_{curr} = \Upsilon_o + (2S/V)N(\sqrt{t}\sqrt{D})/\sqrt{\pi}, \qquad (14)$$

then the diffusion coefficients are 0.5×10^{-16} and 0.1×10^{-16} cm^2 s^{-1}, respectively, for the indicated temperatures. Given that the experimental data on sorption and kinetics were determined with an error of at least 10–15%, the obtained calculated data on the diffusion coefficients should be considered as indicative and for their comparative analysis, similar data are needed for other sorbents with a similar composition, structure, and morphology.

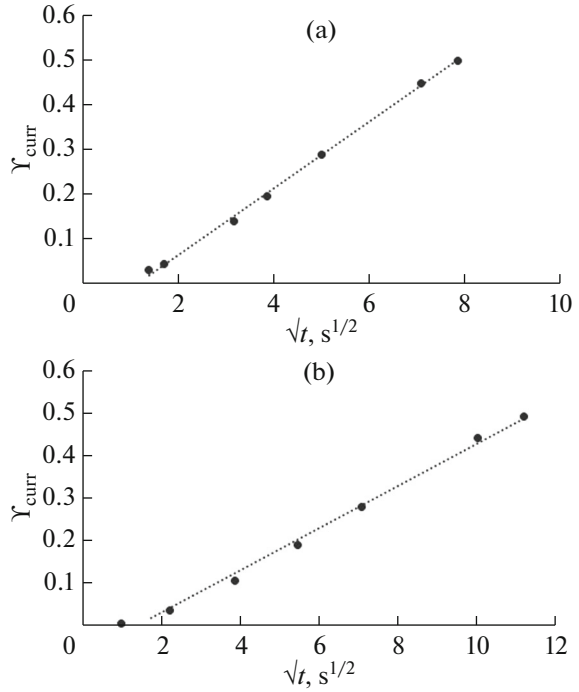

Fig. 8. Dependence of relative value of sorption on $\sqrt{t}$ at: (a) 30, (b) 60°C.

CONCLUSIONS

X-ray amorphous nanostructured lithium aluminosilicate with a specific surface area of 132 m^2 g^{-1} was synthesized. Based on the methods used in the study, the gross formula of the resulting compound was calculated: $Li_{0.63}N_{0.27}Al_{0.9}Si_{2.7}O_8 \cdot 4.7H_2O$. The morphology of the resulting compound and the effect of temperature on its nanotexture were studied, and the formation of nanopores was established after heating of the sample to 900–1000°C. The sorption properties during sorption of Cs^+ ions were studied under static conditions from solutions without a salt background. According to the maximum sorption capacity with respect to Cs^+ ions (4.7 mmol g^{-1}), lithium aluminosilicate is superior to many natural and synthetic sorbents, but to fully characterize the sorbent, we plan to conduct additional research on the influence of the salt background, solution pH, and firing temperature of the aluminosilicate on the sorption properties. The activation energy of the sorption process and the diffusion coefficients of Cs^+ ions at 30 and 60°C have been calculated.

FUNDING

The study was carried out within the state task of the Institute of Chemistry, Far Eastern Branch, Russian Academy of Sciences, FWFN (0205)-2022-0002, topic 2, section 3.

The registration number of the topic in the Plan of the Scientific Council of the Russian Academy of Sciences on Physical Chemistry (section "Adsorption Phenomena") is 22-03-460-05. ICP-MS analysis was performed on equipment of the Center for Shared Use Primorsky Center for Local, Elemental, and Isotope Analysis, Far East Geological Institute, Far Eastern Branch, Russian Academy of Sciences; elemental and XRD analyses were performed on equipment of the Shared Use Center Far Eastern Center for Structural Research, Institute of Chemistry, Far Eastern Branch, Russian Academy of Sciences.

CONFLICT OF INTEREST

The authors of this work declare that they have no conflicts of interest.

REFERENCES

1. Khaleque, A., Alam, M.M., Hoque, M., et al., *Environ. Adv.,* 2020, vol. 2, p. 100019. https://doi.org/10.1016/j.envadv.2020.100019
2. Bhatnagar, A. and Minocha, A.K., *Indian J. Chem. Technol.,* 2006, vol. 13, p. 203.
3. Orlova, A.I. and Ojovan, M.I., *Materials,* 2019, vol. 12, p. 2638. https://doi.org/10.3390/ma12162638
4. Milyutin, V.V., Nekrasova, N.A., and Kaptakov, V.O., *Radioaktivnye Otkhody,* 2020, no. 4, no. 13, p. 80. https://doi.org/10.25283/2587-9707-2020-4-80-89
5. Kwong-Moses, D.S., Elliott, W.C., Wampler, J.M., et al., *J. Environ. Radioact.,* 2020, vol. 211, p. 106074. https://doi.org/10.1016/j.jenvrad.2019.106074
6. Voronina, A.V., Noskova, A.Yu., Semenishchev, V.S., and Gupta, D.K., *J. Environ. Radioact.,* 2020, vol. 217, p. 106210. https://doi.org/10.1016/j.jenvrad.2020.106210
7. Rad, L.R. and Anbia, M., *J. Environ. Chem. Eng.,* 2021, vol. 9, p. 106088. https://doi.org/10.1016/j.jece.2021.106088
8. Abdollahi, T., Towfighi, J., and Rezaei-Vahidian, H., *Environ. Technol. Innovation,* 2020, vol. 17, p. 100592. https://doi.org/10.1016/j.eti.2019.100592
9. Belousov, P., Semenkova, A., Egorova, T., et al., *Minerals,* 2019, vol. 9, p. 625. https://doi.org/10.3390/min9100625
10. Gordienko, P.S., Yarusova, S.B., Shabalin, I.A., et al., *Radiochemistry,* 2014, vol. 56, no. 6, p. 607. https://doi.org/10.1134/S1066362214060058
11. Gordienko, P.S., Shabalin, I.A., Suponina, A.P., et al., *Russ. J. Inorg. Chem.,* 2016, vol. 61, no. 8, p. 946. https://doi.org/10.1134/S003602361608009X
12. Gordienko, P.S., Shabalin, I.A., Yarusova, S.B., et al., *Russ. J. Phys. Chem. A,* 2016, vol. 90, no. 10, p. 2022. https://doi.org/10.1134/S0036024416100125
13. Gordienko, P.S., Shabalin, I.A., Yarusova, S.B., et al., *Theor. Found. Chem. Eng.,* 2018, vol. 52, no. 4, p. 581. https://doi.org/10.1134/S0040579518040127
14. Gordienko, P.S., Shabalin, I.A., Yarusova, S.B., et al., *Russ. J. Inorg. Chem.,* 2019, vol. 64, no. 12, p. 1579. https://doi.org/10.1134/S0036023619120052
15. Yarusova, S.B., Gordienko, P.S., Shichalin, O.O., et al., *Russ. J. Inorg. Chem.,* 2022, vol. 67, no. 9, p. 1386. https://doi.org/10.1134/S0036023622090194
16. Gordienko, P.S., Yarusova, S.B., Shabalin, I.A., et al., *Russ. J. Inorg. Chem.,* 2022, vol. 67, no. 9, p. 1393. https://doi.org/10.1134/S0036023622090042
17. Yarusova, S.B., Shichalin, O.O., Belov, A.A., et al., *Ceram. Int.,* 2022, vol. 48, p. 3808. https://doi.org/10.1016/j.ceramint.2021.10.164
18. Panasenko, A.E., Shichalin, O.O., Yarusova, S.B., et al., *Nucl. Eng. Technol.,* 2022, vol. 54, p. 3250. https://doi.org/10.1016/j.net.2022.04.005
19. Haisheng Hu, Jintao Guo, Meitang Liu, et al., *Hydrometallurgy,* 2022, vol. 213, p. 105929. https://doi.org/10.1016/j.hydromet.2022.105929
20. Helsch, G., Deubener, J., Rampf, M., et al., *J. Non-Cryst. Solids,* 2018, vol. 492, p. 130. https://doi.org/10.1016/j.jnoncrysol.2018.04.031
21. Weihong Zheng, Zipeng Gao, Meng Huang, et al., *J. Non-Cryst. Solids,* 2022, vol. 598, p. 121940. https://doi.org/10.1016/j.jnoncrysol.2022.121940
22. Bejarano-Peña, W.-D., Alcántar-Vázquez, B., and Ramírez-Zamora, R.-M., *Mater. Res. Bull.,* 2021, vol. 141, p. 111353. https://doi.org/10.1016/j.materresbull.2021.111353
23. Qi Zhang, Xiaoli Liang, Dong Peng, and Xuedong Zhu, *Thermochim. Acta,* 2018, vol. 669, p. 80. https://doi.org/10.1016/j.tca.2018.09.002
24. Gordienko, P.S., Shabalin, I.A., Yarusova, S.B., et al., *Russ. J. Phys. Chem. A,* 2019, vol. 93, no. 11. p. 2284. https://doi.org/10.1134/S0036024419110116
25. Timofeev, D.P., *Kinetika adsorbtsii* (Kinetics of Adsorption), Moscow: USSR Acad. Sci., 1962.